

Theory of Polydisperse Block Copolymer Melts: Beyond the Schulz–Zimm Distribution

Nathaniel A. Lynd and Marc A. Hillmyer*,†

Department of Chemistry, University of Minnesota,
Minneapolis, Minnesota 55455

Mark W. Matsen*,‡

Department of Mathematics, University of Reading,
Whiteknights, Reading RG6 6AX, U.K.

Received February 29, 2008

Revised Manuscript Received April 4, 2008

Introduction

Block copolymers are renowned for self-assembling into periodic morphologies with long-range order, and for their rich selection of interesting behaviors and potential applications. There has been a general feeling that this high degree of order requires the block copolymers to have well-defined molecular weights with small polydispersities.¹ However, recent experiments have shown that well-ordered morphologies can be achieved even at high levels of polydispersity.² These observations are important given that many new controlled polymerization methods result in materials with relatively broad molecular weight distributions. To make use of this fact, it is important to understand how the polydispersity affects their phase behavior.

There have been a number of theoretical works^{3–5} investigating the effects of polydispersity on the behavior of block copolymer melts. However, they have all been restricted to polydisperse blocks in which the degree of polymerization, N , follows a unimodal Schulz–Zimm distribution (SZD),⁶

$$p(\sigma) = \frac{k^k \sigma^{k-1} e^{-k\sigma}}{\Gamma(k)} \quad (1)$$

where $\sigma \equiv N/N_n$, $\Gamma(k)$ is the standard Gamma function, and k is a parameter that determines the polydispersity index, PDI $\equiv N_w/N_n = (1 + k)/k$. The SZD is used primarily because it has a simple functional form that spans the monodisperse distribution (PDI = 1) and the *most probable* distribution (PDI = 2). When the SZD is assumed, the standard AB diblock copolymer melt acquires just two more parameters, PDI_A and PDI_B, in addition to the conventional quantities of composition, $f \equiv (N_A)_n/N_n$, and segregation, χN_n , where χ is the usual Flory–Huggins interaction parameter and $N_n \equiv (N_A)_n + (N_B)_n$ is the total degree of polymerization. The danger of this limited approach is that it propagates a general attitude that polydispersity effects are almost entirely dictated by PDI_A and PDI_B.

In this Note, we compare the SZD to a realistic distribution obtained from a numerical simulation for the kinetics of an equilibrium polymerization like that of D,L-lactide.⁷ Then we test how this distribution impacts the phase behavior of AB diblock copolymers with a polydisperse A block and a mono-disperse B block, using numerical self-consistent field theory (SCFT).⁸ In doing so, we find that some quantitative effects of polydispersity are significantly altered when the SZD is replaced by our simulated equilibrium polymerization distribution (EPD) of the same polydispersity index, PDI_A.

Kinetics of an Equilibrium Polymerization

The synthesis of a polymer generally begins with an initiation event, where the first monomer attaches to an initiator, and it is followed by a large number of propagation events, each adding another monomer to the chain. In most polymerizations, the propagation events are essentially irreversible, and thus depropagation can be ignored. In an equilibrium polymerization, on the other hand, depropagation events contribute to the overall kinetics. At the equilibrium monomer concentration, the rates of propagation and depropagation are equal and monomers are continuously joining to and detaching from the active end of each chain.⁹ Miyake and Stockmayer¹⁰ were the first to model this type of polymerization using the set of coupled equations,

$$\frac{dI}{dt} = -k_i MI + k_{-i} P_1 \quad (2)$$

$$\frac{dM}{dt} = -k_i MI - k_p MP + k_{-i} P_1 + k_{-p}(P - P_1) \quad (3)$$

$$\frac{dP_1}{dt} = -k_p MP_1 + k_i MI + k_{-p} P_2 - k_{-i} P_1 \quad (4)$$

$$\frac{dP_N}{dt} = k_p M(P_{N-1} - P_N) + k_{-p}(P_{N+1} - P_N) \quad (5)$$

where $I(t)$, $M(t)$, and $P_N(t)$ are the concentrations of initiator, monomer, and polymers of polymerization N , respectively, and $P(t) = \sum_N P_N(t)$. The parameters k_i and k_{-i} are the forward and reverse rate constants for the initiation event, while the rate constants k_p and k_{-p} are for the propagation and depropagation of monomers. An analytical solution does not generally exist, and so the equations have to be integrated numerically, which we do using the fifth-order accurate Runge–Kutta algorithm.¹¹ Results are shown in Figure 1a for a reaction starting from $M(0) \equiv M_0 = 1$ mol/L and $I(0) \equiv I_0 = 0.01$ mol/L.

Our simulation assumes that k_i is extremely large while $k_{-i} = 0$, which implies that all the initiator is immediately consumed such that $I(t) = 0$ and $P(t) = I_0$ for all $t > 0$. For the following time of $t \lesssim t_p \equiv 1/k_p I_0 = 100$ s, the depolymerization is negligible and the monomer concentration decreases as

$$M(t) = (M_0 - I_0)e^{-t/t_p} \quad (6)$$

This exponential decay is shown in Figure 1a with a dotted curve. During this period, the polymers develop a Poisson distribution,

$$P_N(t) = I_0 e^{-\nu} \frac{\nu^{(N-1)}}{(N-1)!} \quad (7)$$

where

$$\nu(t) = \frac{M_0 - I_0}{I_0} (1 - e^{-t/t_p}) \quad (8)$$

is the average number of monomers added to each of the $P = I_0$ chains following the initial consumption of the initiator (i.e., $N_n = 1 + \nu$). The resulting polydispersity index,

$$\text{PDI} = 1 + \frac{\nu}{(1 + \nu)^2} \quad (9)$$

is shown in Figure 1a with a dotted curve. Once $M(t)$ decreases sufficiently, the depolymerization begins to balance the polymerization, and N_n saturates. However, N_w continues to increase, and the PDI of the distribution rises toward 2.0. Parts b and c

* Corresponding author.

† E-mail: hillmyer@umn.edu.

‡ E-mail: m.w.matsen@reading.ac.uk.

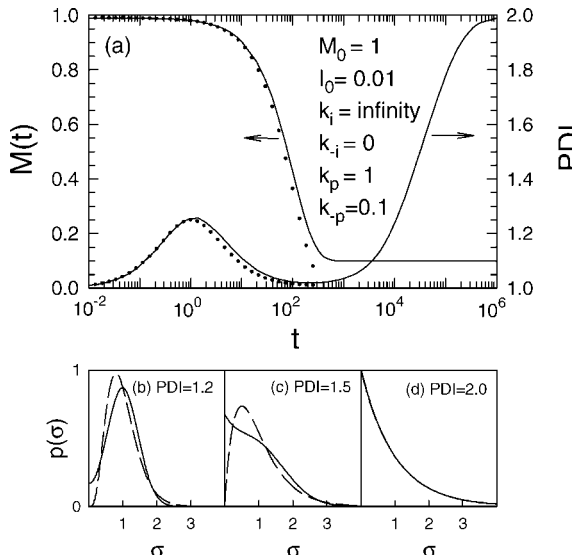


Figure 1. (a) Monomer concentration, $M(t)$, in units of mol/L and polydispersity index, PDI, during an equilibrium polymerization plotted logarithmically as a function of time in units of seconds. The dotted curves denote the approximations in eqs 6 and 9. The small plots below compare the resulting EPD (solid curves) to the SZD of eq 1 (dashed curves) at (b) PDI = 1.2, (c) PDI = 1.5, and (d) PDI = 2.0.

of Figure 1 compare the resulting EPD with the SZD at PDI = 1.2 and 1.5, respectively.

Although we cannot run our simulation to $t = \infty$, the limit is easily obtained by solving eqs 2–5 with $I = 0$, $M = M_{\text{eq}}$, and all the derivatives set to zero. The equilibrium value of the monomer concentration has to be adjusted so that $N_n = (M_0 - M_{\text{eq}})/I_0$, which for our chosen rate constants gives $M_{\text{eq}} = 0.0989$ mol/L. The $t = \infty$ distribution, shown in Figure 1d, has PDI = 1.9889 and is nearly indistinguishable from the most probable distribution for which PDI = 2.0; the small difference results due to the finite size of N_n .

Domain Spacing

Now we turn our attention to AB diblocks, where the number of A segments in each molecule, $N_A = \alpha f N_n$, involves the random variable, σ , with distribution, $p(\sigma)$, but the number of B segments is fixed at $N_B = (1 - f)N_n$. We begin by examining the equilibrium domain spacing for melts of symmetric composition, $f = 0.5$, where the preferred morphology is the lamellar phase. The calculations are performed using the SCFT algorithm developed in ref 4, where averages over the SZD are performed by the Gaussian quadrature method; the algorithm is so efficient that the necessary averages over the EPD can be handled by explicitly summing over the thousand or so values of N , where $P_N \gtrsim 10^{-10}$ mol/L. Figure 2 shows the resulting lamellar period, D , of polydisperse diblocks relative to that, D_0 , of monodisperse diblocks as a function of polydispersity, PDI_A . As demonstrated previously by both theory^{4,12} and experiment,⁷ the polydispersity causes an increase in the domain spacing. However, it is now evident that the magnitude of the increase is significantly affected by the detailed shape of the distribution; in this case, the EPD (solid curves) produces a much larger increase than the SZD (dashed curves) at equivalent PDI_A . Naturally, the difference in D is most pronounced when the difference in the distributions is greatest (i.e., $\text{PDI}_A \approx 1.5$). Note that even though the EPD and SZD curves in Figure 2 approach each other as $\text{PDI}_A \rightarrow 2.0$, there is a small but visible mismatch due to the

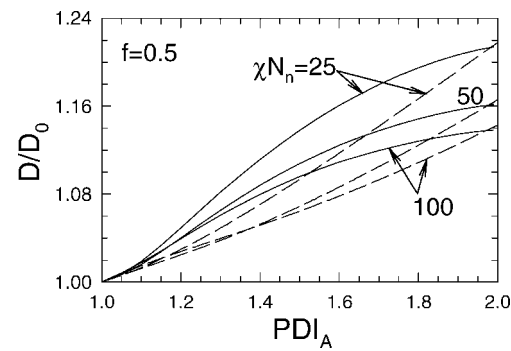


Figure 2. Relative domain spacing, D/D_0 , as a function of A-block polydispersity, PDI_A , using the EPD (solid curves) and the SZD (dashed curves) at $f = 0.5$ and $\chi N_n = 25$, 50, and 100.

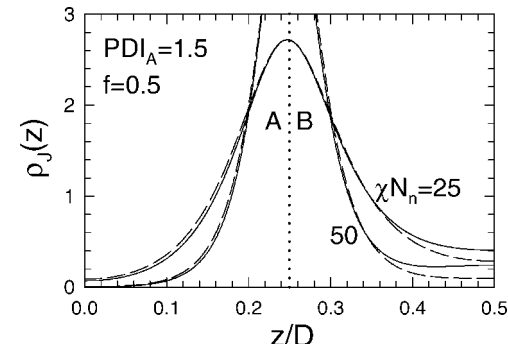


Figure 3. Junction distribution, $\rho_j(z)$, from the center of an A domain at $z = 0$ to the center of a B domain at $z = D/2$, plotted for a polydispersity of $\text{PDI}_A = 1.5$, a composition of $f = 0.5$, and segregations of $\chi N_n = 25$ and 50. Solid and dashed curves denote results for the EPD and SZD, respectively, and the dotted line marks the interface at $z = D/4$.

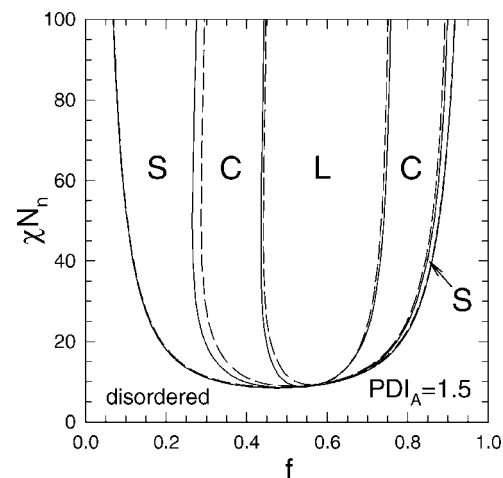


Figure 4. Phase diagram for the classical lamellar (L), cylindrical (C), and spherical (S) phases. The order-order transitions are calculated using a unit-cell approximation and ignoring two-phase coexistence, while the order–disorder transition is estimated by the disordered-state spinodal curve. Solid and dashed curves denote results for the EPD and SZD, respectively.

slight difference mentioned above between the $t \rightarrow \infty$ limit of the EPD and the most probable distribution.

One contributing factor for the increase in domain spacing is that the polydispersity decreases the entropic elasticity of the A-rich domain. Simply put, the longer A-blocks can fill the center of their domain without having to stretch so much, and thus less configurational entropy is lost for a give domain

thickness. According to strong-stretching theory (SST),^{4,13} the elastic energy of the A-domain is reduced by the factor,

$$S_A \equiv \int_0^\infty d\sigma [1 - \int_0^\sigma d\sigma' p(\sigma')]^3 \quad (10)$$

which causes a change in the lamellar spacing of

$$\frac{D}{D_0} = [fS_A + 1 - f]^{-1/3} \quad (11)$$

At $PDI_A = 1.5$, the EPD gives $S_A = 0.437$, leading to an expansion of $D/D_0 = 1.117$, whereas the SZD gives $S_A = 0.482$ leading to $D/D_0 = 1.105$. However, this is a much smaller difference than observed in our SCFT calculations at finite segregation (e.g., only 40% of the difference predicted at $\chi N_n = 100$).

For finite values of χN_n , there is an additional effect where polymers with short A blocks detach from the interface and swell the B-rich domain. In effect, the polymers at small $\sigma \equiv N_A/fN_n \lesssim \sigma_{cr}$ behave as a B-type homopolymer rather than a diblock copolymer. The *critical* value, below which short A blocks pull out of their domain, is estimated by

$$\sigma_{cr} = \frac{1}{\chi N_n f} \left[\frac{2aN_n^{1/2}}{D_0} \sqrt{\frac{\chi N_n}{6}} + \frac{\pi^2(1-f)D_0^2}{32a^2N_n} \right] \quad (12)$$

obtained by balancing the increased energy of placing $\sigma_{cr}fN_n$ A segments in the B domain with the energy saved by removing a junction from the interface and allowing the B block to relax.⁴ This expression provides $\sigma_{cr} = 0.217, 0.137$, and 0.086 for $\chi N_n = 25, 50$, and 100, respectively,¹⁴ and approaches zero monotonically as $\chi N \rightarrow \infty$. We can see from Figure 1c for $PDI_A = 1.5$ that the EPD has significantly more diblocks with $\sigma \lesssim \sigma_{cr}$ than does the SZD, and thus we expect a much larger population of chains to detach from the interface. This is confirmed in Figure 3, where the distribution of junction points, $\rho_j(z)$, is plotted from the middle of an A domain to the middle of a neighboring B domain. While most junction points are located near the interface (dotted line), the *pull-out* of short A blocks from their domain causes a significant population of junction points in the middle of the B domain, which is about twice as large for the EPD.

Phase Diagram

Next, we examine the phase diagram, focusing on $PDI_A = 1.5$ where the difference in the EPD and SZD is approximately greatest. For computational efficiency as well as clarity, we invoke several simplifying approximations. First, we limit our attention to the classical phases [i.e., lamellar (L), cylindrical (C), and spherical (S)], which allows us to implement the standard unit-cell approximation (UCA).¹⁵ Second, we ignore the two-phase coexistence regions that separate the single-phase regions, which in any case are generally narrow for $PDI_A = 1.5$.⁵ The one exception is the order-disorder transition (ODT), where the period of S diverges if we attempt to calculate the boundary without considering the two-phase coexistence region. Therefore, we estimate the ODT by the spinodal curve, where the peak in the disordered-state scattering function, $S(q)$,¹⁶ diverges.

Figure 4 compares the resulting phase diagram for the EPD (solid curves) and the SZD (dashed curves); the differences are rather minimal. We have also performed a few SCFT calculations without the UCA in order to assess the impact on the complex phases; the shift in the gyroid region is similarly small¹⁷ and the perforated-lamellar phase remains metastable for both distributions. It is somewhat surprising how little the phase diagram is affected given the sizable change in domain spacing

caused by the change in distributions. This is because the two effects, the reduction in domain elasticity and the increased pull-out of short A blocks, acted together to increase D whereas this time they produce opposite trends that approximately cancel out. On one hand, the reduced elasticity of the A domain favors A blocks on the inside of interfacial curvature, thus shifting the phase boundaries to larger f .^{5,12} On the other hand, the swelling of the B domain by the polymers with short A blocks (i.e., $\sigma \lesssim \sigma_{cr}$) tends to shift the phase boundaries to smaller f .^{15,18}

Conclusions

We have compared the effects of polydispersity on the phase behavior of block copolymer melts for two distinct distributions, EPD and SZD. Even when the polydispersity indices were perfectly matched, there were sizable differences in the degree to which the entropic elasticity of the polydisperse domain was affected and in the number of polymers that detached from the interface. In our particular study, the combination of these effects had a large impact on the domain spacing, but a rather negligible result on the phase diagram. The interplay between these two effects is reasonably complicated, and there is no doubt that consideration of the entire molecular weight distribution, and not just its PDI, is important for understanding the influence of polydispersity on block copolymer phase behavior.

Acknowledgment. This work was supported in part by the MRSEC Program of the National Science Foundation, under Award Number DMR-0212302, and in part by the EPSRC, under Grant Number EP/E010342/1.

References and Notes

- (1) Hillmyer, M. A. *J. Polym. Sci., Part B* **2007**, *45*, 3249.
- (2) Lynd, N. A.; Meuler, A. J.; Hillmyer, M. A. *Prog. Polym. Sci.* Submitted for publication.
- (3) (a) Leibler, L.; Benoit, H. *Polymer* **1981**, *22*, 195. (b) Hong, K. M.; Noolandi, J. *Polym. Commun.* **1984**, *25*, 265. (c) Burger, C.; Ruland, W.; Semenov, A. N. *Macromolecules* **1990**, *23*, 3339. (d) Erukhimovich, I.; Dobrynin, A. V. *Macromol. Symp.* **1994**, *81*, 253. (e) Sides, S. W.; Frederickson, G. H. *J. Chem. Phys.* **2004**, *121*, 4974. (f) Jiang, Y.; Chen, T.; Ye, F.; Liang, H.; Shi, A.-C. *Macromolecules* **2005**, *38*, 6710. (g) Jiang, Y.; Yan, X.; Liang, H.; Shi, A.-C. *J. Chem. Phys. B* **2005**, *109*, 21047. (h) Jiang, Y.; Huang, R.; Liang, H. *J. Chem. Phys.* **2005**, *123*, 124906.
- (4) Matsen, M. W. *Eur. Phys. J. E* **2006**, *21*, 199.
- (5) Matsen, M. W. *Phys. Rev. Lett.* **2007**, *99*, 148304.
- (6) (a) Schulz, G. V. *Z. Phys. Chem.* **1939**, *B43*, 25. (b) Zimm, B. H. *J. Chem. Phys.* **1948**, *16*, 1099.
- (7) (a) Lynd, N. A.; Hillmyer, M. A. *Macromolecules* **2005**, *38*, 8803. (b) Lynd, N. A.; Hillmyer, M. A. *Macromolecules* **2007**, *40*, 8050.
- (8) Matsen, M. W. *J. Phys.: Condens. Matter* **2002**, *14*, R21.
- (9) Strictly speaking, nearly all monomers polymerize via an equilibrium process since ΔH and ΔS of the polymerization are typically both negative.
- (10) Miyake, A.; Stockmayer, W. H. *Makromol. Chem.* **1965**, *88*, 90.
- (11) Press, W. H.; Teukolsky, S. A.; Vetterling, W. T.; Flannery, B. P. *Numerical Methods in C++: The Art of Scientific Computing*, 2nd ed.; Cambridge University Press: New York, 2005.
- (12) Cooke, D. M.; Shi, A.-C. *Macromolecules* **2006**, *39*, 6661.
- (13) Milner, S. T.; Witten, T. A.; Cates, M. E. *Macromolecules* **1989**, *22*, 851.
- (14) These values of σ_{cr} are calculated using the SST estimate of D_0 from the Appendix of ref 4.
- (15) Matsen, M. W. *Macromolecules* **2003**, *36*, 9647.
- (16) The calculation of $S(q)$ is nicely described in Appendix A of ref 12, but there are several typographical errors. The f_A 's in the denominators of eqs A3 and A4 should be removed, and the polydisperse A domain is handled by substituting $f_A \rightarrow f_A \sigma$ and averaging S_{AA} and S_{AB} with respect to $p(\sigma)$.
- (17) At $\chi N = 20$, canonical SCFT calculations without the UCA predict the gyroid phase boundaries to occur at $f = 0.4175, 0.4480, 0.6842$, and 0.7099 for the EPD, as compared to $f = 0.4271, 0.4582, 0.6806$, and 0.7066 for the SZD.
- (18) Matsen, M. W. *Macromolecules* **1995**, *28*, 5765.